Materials Science & Engineering A 625 (2015) 28–35

Contents lists available at ScienceDirect

Materials Science & Engineering A

journal homepage: www.elsevier.com/locate/msea

Experiments and crystal plasticity finite element simulations of nanoindentation on Ti–6Al–4V alloy

Fengbo Han [a], Bin Tang [a,*], Hongchao Kou [a], Jinshan Li [a], Yong Feng [a,b]

[a] State Key Laboratory of Solidification Processing, Northwestern Polytechnical University, Xi'an 710072, PR China
[b] Western Superconducting Technologies Co., Ltd., Xi'an 710018, PR China

ARTICLE INFO

Article history:
Received 12 August 2014
Received in revised form
26 November 2014
Accepted 26 November 2014
Available online 5 December 2014

Keywords:
Nanoindentation
Crystal plasticity
Finite element method
Titanium alloy

ABSTRACT

In this paper, we investigated the micromechanical behavior of Ti–6Al–4V by means of nanoindentation experiments performed on a specimen with duplex microstructure. After nanoindentation experiments, electron backscattered diffraction (EBSD) scan was conducted on the nanoindentation region to obtain the crystallographic information. Then the crystal plasticity finite element (CPFE) simulations were carried out using the measured grain orientations. The simulated load–displacement curves match the experimental data well with proper model parameters. It was found that the hardness varied with the grain orientation, and the pileup patterns on the indented surfaces exhibit significant anisotropy and grain orientation dependence. The effects of grain boundary and orientation of Berkovich indenter on the nanoindentation results were discussed.

1. Introduction

Nanoindentation is an important tool for measuring the mechanical properties of materials at small scale, and the indentation depth can range from just a few tenths of nanometers to over one micrometer [1]. This method has been used extensively by researchers [2–6] around the world to study elastic modulus, hardness, size effects, sinking-in and piling-up etc. Many simulation works on nanoindentation have also been carried out to study the effect of factors on the plastic anisotropy of various materials during indentation [7–11], in which the crystal plasticity finite element (CPFE) models were usually adopted. In the past few decades, the CPFE method has achieved great success in simulating the plastic deformation process of different crystalline materials, for example see [12–15]. Nanoindentation is a complicated deformation process due to the complex stress conditions in the region underneath the indenter that produce non-uniform strain [4], and it is difficult to analyze the detailed deformation mechanism of the inner region beneath the sample surface, while the CPFE simulation can give a fairly comprehensive understanding of the nanoindentation process.

Ti–6Al–4V is a common $\alpha+\beta$ titanium alloy that is used in a variety of structural engineering applications such as medical implants and turbine blades. Due to its low density and attractive mechanical and corrosion resistant properties [16–18], Ti–6Al–4V has been one of the most important and widely used titanium alloys in aerospace industries. Therefore, great attention has been given in many aspects to study the behavior of Ti–6Al–4V alloy, including flow behavior and microstructural mechanisms during hot working [19,20], microstructure evolution during heat treatment [21], and the superplastic deformation ability [22]. Although some researchers have investigated micromechanical behavior of Ti–6Al–4V alloy by nanoindentation [4] and microindentation [23–25], there is no simulation study of nanoindentation on this alloy.

The purpose of the present study is to investigate nanoindentation and micromechanical behavior of Ti–6Al–4V alloy by combining experiments and CPFE simulations. The remainder of this paper is organized as follows: Section 2 gives a description of the experimental procedure. Section 3 is devoted to description of the crystal plasticity constitutive model and the finite element implementation. Section 4 gives the experimental results and the CPFE simulation results of nanoindentation and discussion. Finally, conclusions are summarized in Section 5.

2. Experiments

The Ti–6Al–4V alloy used in the present study was heat-treated to a duplex microstructure containing equiaxed primary α grains and lamellar structure, and the optical micrograph of the specimen is shown in Fig. 1. The volume fraction of the β phase is rather small, 0.07–0.08, and they are dispersed between acicular α laths.

* Corresponding author. Tel.: +86 29 88460568; fax: +86 29 88460294.
E-mail address: toby@nwpu.edu.cn (B. Tang).

http://dx.doi.org/10.1016/j.msea.2014.11.090
0921-5093/

The sample was ground with sand paper, then was polished with 1.5 μm and 0.5 μm diamond to mirror finish. In order to achieve the surface quality required for nanoindentation test and EBSD examination, the sample was electropolished with a solution of 5% perchloric acid in alcohol using a voltage of 30 V for 240 s at 25 °C. Nanoindentation tests were conducted in an CSM nanoindentation tester equipped with a Berkovich diamond indenter at room temperature under the laboratory environment. We chose 5 s loading to the maximum load (2000 μN), 2 s resting and 5 s unloading. After an array of nanoindents was made, the sample was analyzed in a ZEISSSUPRA55-SEM operating at 20 kV and equipped with a Nordlys EBSD detector and the TSLOIM EBSD software. The surface topography around nanoindent was measured by Bruker Dimension® Icon™ AFM.

3. Crystal plasticity finite element method

3.1. Crystal plasticity constitutive model

In this work, the CPFE frame and method based on the works of Asaro and Needleman [26] and Peirce et al. [27] is employed, and it has been used in [6,12,28]. The crystal orientation and the activated slip systems are taken into account in the model. The total deformation gradient **F** of finite strain can be expressed by polar decomposition

$$\mathbf{F} = \mathbf{F}^e\mathbf{F}^p \tag{1}$$

where $\mathbf{F}^e$ represents the elastic deformation gradient which is composed of the elastic stretching and rigid body rotation of the configuration, and $\mathbf{F}^p$ denotes the plastic shear due to slip. The plastic velocity gradient $\mathbf{L}^p$ is defined as

$$\mathbf{L}^p = \dot{\mathbf{F}}^p(\mathbf{F}^p)^{-1} = \sum_{\alpha=1}^{N} \dot{\gamma}^\alpha \mathbf{s}^\alpha \otimes \mathbf{n}^\alpha \tag{2}$$

where $\dot{\gamma}^\alpha$, $\mathbf{s}^\alpha$ and $\mathbf{n}^\alpha$ are shear strain rate, slip direction vector and the normal vector to the slip plane of any given slip system α, respectively. N is the number of the active slip systems. The shear strain rate $\dot{\gamma}^\alpha$ of the αth slip system is determined by a simple rate-dependent power law relation proposed by Hutchinson [29] as follows:

$$\dot{\gamma}^\alpha = \dot{\gamma}_0^\alpha \left|\frac{\tau^\alpha}{g^\alpha}\right|^n \mathrm{sgn}(\tau^\alpha) \tag{3}$$

where $\dot{\gamma}_0^\alpha$ is the reference strain rate, τ^α is the resolved shear stress, g^α is the slip system strength or resistance to shear, and n is the inverse strain rate sensitivity exponent. Due to the accumulation of dislocations, strain hardening will occur, and is characterized by the evolution of the rate of change of yield strengths given by

$$\dot{g}^\alpha = \sum_\beta h_{\alpha\beta}\dot{\gamma}^\beta \tag{4}$$

where $h_{\alpha\beta}$ is the matrix of slip hardening moduli. The hardening model of Asaro and Needleman [26], Pierce et al. [27] is used here, and the self-hardening moduli is expressed as

$$h_{\alpha\alpha} = h(\gamma) = h_0 \mathrm{sech}^2\left|\frac{h_0\gamma}{\tau_s - \tau_0}\right| \tag{5}$$

where h_0 is the initial hardening modulus, τ_0 is the initial value of the yield strength, τ_s is the saturation value, and γ is the Taylor cumulative shear strain on all the activated slip systems, which is given by

$$\gamma = \sum_\alpha \int_0^t |\dot{\gamma}^\alpha| dt \tag{6}$$

The latent hardening moduli are given by

$$h_{\alpha\beta} = qh(\gamma) \quad (\alpha \neq \beta) \tag{7}$$

where q is the latent hardening parameter.

3.2. Finite element implementation

The crystal plasticity constitutive model was incorporated into the implicit finite element code ABAQUS/Standard through the user material subroutine (UMAT). The subroutine updates the stress state and the solution dependent state variables and provides the material Jacobian matrix.

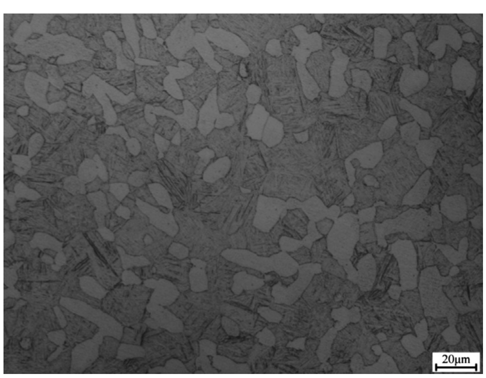

Fig. 1. Microstructure of the Ti–6Al–4V alloy.

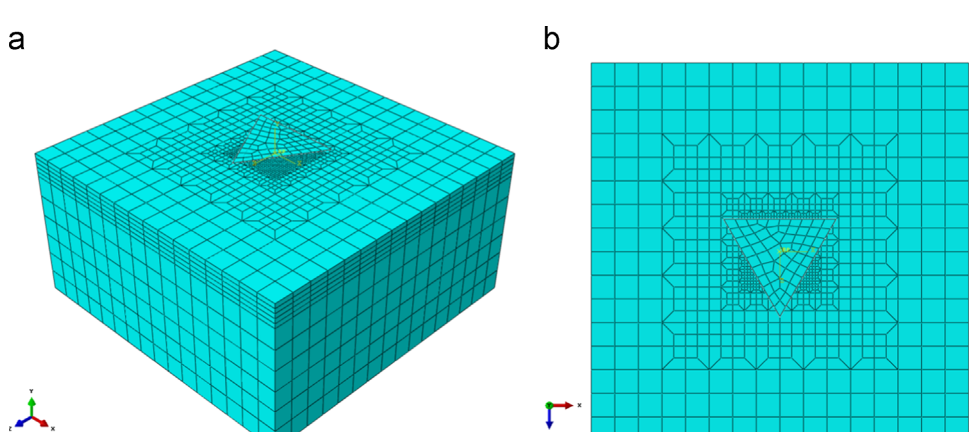

Fig. 2. Nanoindentation model setup.